Plant Physiology and Biochemistry 149 (2020) 50–60

Contents lists available at ScienceDirect

Plant Physiology and Biochemistry

journal homepage: www.elsevier.com/locate/plaphy

Research article

Foliar application of nanoparticles mitigates the chilling effect on photosynthesis and photoprotection in sugarcane

Nabil I. Elsheery[a,b,1], V.S.J. Sunoj[a,1], Y. Wen[a], J.J. Zhu[a], G. Muralidharan[a], K.F. Cao[a,*]

[a] State Key Laboratory of Conservation and Utilization of Subtropical Agro-bio-resources and Guangxi Key Laboratory of Forest Ecology and Conservation, College of Forestry, Guangxi University, Nanning, 530004, Guangxi, PR China
[b] Department of Agricultural Botany, Tanta University, Tanta, 72513, Egypt

ARTICLE INFO

Keywords:
Sugarcane
Nanoparticles
Chilling tolerance
Gas exchange
Photoprotection

ABSTRACT

Chilling is one of the main abiotic stresses that adversely affect the productivity of sugarcane, in marginal tropical regions where chilling incidence occurs with seasonal changes. However, nanoparticles (NPs) have been tested as a mitigation strategy against diverse abiotic stresses. In this study, NPs such as silicon dioxide ($nSiO_2$; 5–15 nm), zinc oxide (nZnO; < 100 nm), selenium (nSe; 100 mesh), graphene (graphene nanoribbons [GNRs] alkyl functionalized; 2–15 μm × 40–250 nm) were applied as foliar sprays on sugarcane leaves to understand the amelioration effect of NPs against negative impact of chilling stress on photosynthesis and photoprotection. To this end, seedlings of moderately chilling tolerant sugarcane variety Guitang 49 was used for current study and spilt plot was used as statistical design. The changes in the level chilling tolerance after the application of NPs on Guitang 49 were compared with tolerance level of chilling tolerant variety Guitang 28. NPs treatments reduced the adverse effects of chilling by maintaining the maximum photochemical efficiency of PSII (F_v/F_m), maximum photo-oxidizable PSI (P_m), and photosynthetic gas exchange. Furthermore, application of NPs increased the content of light harvesting pigments (chlorophylls and cartinoids) in NPs treated seedlings. Higher carotenoid accumulation in leaves of NPs treated seedlings enhanced the nonphotochemical quenching (NPQ) of PSII. Among the NPs, $nSiO_2$ showed higher amelioration effects and it can be used alone or in combination with other NPs to mitigate chilling stress in sugarcane.

1. Introduction

The climate change leads to alterations in rainfall pattern and sea levels, accompanied by the occurrence of extreme weather events, such as low and high temperatures, droughts, cyclones and floods (Trenberth et al., 2007; Dhillon and Wuehlisch, 2013; IPCC, 2013). These catastrophic incidents can adversely affect crop productivity in different regions of the world (Lobell, 2008; Sunoj et al., 2016), including tropical and subtropical regions (Hong and Li, 2001; Cao et al., 2006; Elsheery et al., 2007, 2008).

Sugarcane (*Saccharum officinarum* L.) is a major C4 crop predominantly cultivated in tropical and subtropical regions and is a vital industrial crop used for versatile purposes, such as sugar and bioenergy (alcohol) production, manure for alkaline and saline soil, fodder for cattle and paper production. At the same time, chilling incidence caused severe damage to sugarcane productivity in countries located in marginal tropical and subtropical regions (Selvarajan et al., 2018). The optimum growth temperature for the highest sugar yield is 25 °C–30 °C and suboptimum growth temperature conditions (below 15 °C–12 °C) diminishes the growth rate, sugar yield, and biomass production of sugarcane (Ebrahim et al., 1998; Li et al., 2015; Li and Yang, 2015).

China is in the third position, after Brazil and India, among the top 10 sugarcane producing countries in the world with an annual sugar production of 104.4 mt, which accounts for 5.8% of the total global production (FAO, 2017; Factfish, 2015). Recently, extreme weather occurrences in the form of chilling (below 10 °C) and frost (below 0 °C) incidence have become more frequent and severe in southern China, which adversely affects sugarcane production (Li and Yang, 2015; Li et al., 2015). During the winter of 2008, chilling incidence caused 68.03% crop loss in sugarcane growing areas of central Guangxi, China, and the occurrence of such deleterious events are predicted to be more frequent in these areas in near future due to climate change (IPCC, 2013). Such circumstances necessitate new mitigation strategies to prevent chilling or frost damage to the sugarcane production in the

* Corresponding author.
E-mail address: kunfangcao@gxu.edu.cn (K.F. Cao).
[1] Authors are equally contributed in this work.

https://doi.org/10.1016/j.plaphy.2020.01.035
Received 23 October 2019; Received in revised form 27 January 2020; Accepted 28 January 2020
Available online 31 January 2020

Abbreviations

Y(NPQ)	Effective quantum yield of regulated non-photochemical quenching
Y(NO)	Yield of non-regulated heat dissipation of PSII
Y(I)	Effective photochemical quantum yield of PSI
Y(II)	Effective photochemical quantum yield of PSII
Y(ND)	Donor side limitation of PSI
Y(NA)	Acceptor side limitation of PSI
F_v/F_m	Maximum quantum yield of PSII in the dark-adapted state
P_m	Maximum photo-oxidizable PSI
ETR I	Photosynthetic electron flow through PSI
ETR II	Photosynthetic electron flow through PSII
Y(CEF)	Effective quantum yield of CEF
LEF	Linear electron flow
PAR	Photosynthetic active radiation
P_N	Photosynthesis
Gs	Stomatal conductance
C_i	Internal CO_2 concentration
CE	Carboxylation capacity
NPs	Nanoparticles
$nSiO_2$	Nano silicon dioxide
nZnO	Nano zinc oxide
nSe	Nano selenium
GNRs	Nano graphene

future.

To mitigate the different stress factors, new advanced agricultural technologies need to be invented and implemented. Currently, the main target of agricultural technologies and practices is to increase crop productivity, climatic hazards which occur unpredictably and cause serious damage to crop production are not often considered. At the same time, implementation of these new technologies, along with the high cost of irrigation and fertilizers, negatively influences the economic stability of farmers, which threatens global food security, particularly in developing counties. To solve this concern, new low cost techniques will be useful for famers. Nanoparticles (NPs) have been found to have a great potential application in agriculture (Azimi et al., 2014). Using NPs which are available in nature or synthesised from natural occurring materials can reduce the higher production cost NPs and can be an effective solution for famers to improve productivity and enhance stress tolerance of crops (Gui et al., 2015; Perez-de-Luque, 2017; Guo et al., 2019).

Furthermore, many researchers used NPs against diverse abiotic stress factors such as salinity (Siddiqui et al., 2014; Abdel Elatef et al., 2016; Abdelhielim et al., 2017; Yasen et al., 2017; Husain and Abu-Baker, 2018), drought (Ashkavand et al., 2015; Mahdavi et al., 2016), heat (Qi et al., 2013; Haghighi et al., 2104) and metal toxicity (Li and Huang, 2014; Singh and Lee, 2016; Guo et al., 2019). On the other hand, to the best of our knowledge, no previous study has reported on the application of NPs to ameliorate tolerance to mitigate the impact of chilling on sugarcane.

In several crops, under abiotic stress conditions, application of NPs significantly increases plant height, root length, root volume, biomass accumulation, plant nutrient status, and photosynthetic rate as compared to the respective controls (Stampoulis et al., 2009; Ma et al., 2010; Burklew et al., 2012; Alidoust and Isoda, 2013; Haghighi et al., 2014; El-Ramady et al., 2015; Karimi and Mohsenzadeh, 2016; Guo et al., 2019). On the other hand, down-regulation of photosynthesis under stress conditions reduces growth, development, and productivity of crops (Sunoj et al., 2016, 2017). Furthermore, previous studies have reported that chilling in marginal tropical and subtropical regions negatively affect photosynthesis of plant species (Elsheery et al., 2008; Huang et al., 2010) and promising amelioration capacity expressed by NPs can be implemented as mitigation strategy for protecting chilling stress.

Reduction in photosynthesis of crops under chilling is a result of photoinhibition of photosystems (PSII and PSI) in the thylakoid membrane of chloroplasts, which can occur due to stomatal and nonstomatal limitations, and results in electron overload on photosystems (Allan and Orts, 2001; Huang et al., 2016a,b). Photoinhibition or photodamage of photosystems consequences in the accumulation of reactive oxygen species (ROS) that damages DNA, proteins and lipids (Tjus et al., 1998; Miyake, 2010). Moreover, damage to the thylakoid membrane lipids increases membrane fluidity, causing total destruction of photosynthetic apparatuses (Elsheery et al., 2008) . At the same time, activation of photoprotection mechanisms can effectively manage the excess energy before the production of excess ROS, by proper removal of ROS, which include: (1) non-photochemical quenching (NPQ) to dissipate excess absorbed light energy, (2) cyclic electron flow (CEF) around PSI, and (3) alternative electron flow (water-water cycle [WWC] or the Mehler–ascorbate peroxidase pathway [MAP]) (Miyake, 2010; Neto et al., 2017).

Previous studies have revealed that foliar application of NPs cause a reduction in ROS (Burman et al., 2013) by increasing enzymatic quenching of ROS (enzymatic activities of superoxide dismutase [SOD], catalase [CAT] and peroxidase [POD]), and thereby mitigates phytotoxicity in plants (Kim et al., 2012; Karimi and Mohsenzadeh, 2016), which is important to prevent photoinhibition and further photodamage by managing the electron flow between photosystems. To the best of our knowledge, no previous study has monitored the effect of NPs on efficient light energy utilization and photoprotection mechanisms; therefore, there exists limited information on the targeting areas of particular NPs that could be helpful for the formulation of consortiums of different NPs.

Hence, the main aim of this study was to understand the amelioration capacity of different NPs foliar applications for chilling tolerance in sugarcane, with a special focus on gas exchange and light energy utilization and dissipation. Furthermore, we aimed to identify the best NPs that can improve the photosynthesis and photoprotection mechanisms of sugarcane under chilling.

2. Materials and methods

2.1. Plant materials and growth conditions

The experiment was carried out from December 2018 to January 2019 in an open field of a nursery on the campus of Guangxi University, Nanning, China (22.83°N, 108.28°E). Newly released, moderately chilling tolerant variety Guitang 49 and chilling tolerant variety Guitang 28 were selected and planted in pots (width 33 cm × height 30 cm) filled with soil. Both varieties were developed by Guangxi

Table 1
The chemical analysis of applied soil.

Parameters	Organic matter	Total N	Total P	Total K	Hydrolytic N	available P	Available K	Soil pH
Value	19.65 g/Kg	0.10%	0.04%	0.62%	86 mg/g	4.7 mg/kg	74 mg/kg	5.7

Sugarcane Research Institute, Guangxi Academy of Agricultural Sciences, China. The chemical analysis of applied soil presented in Table (1). Guitang 28 was used to compare the effect of NPs in enhancing the chilling tolerance of Guitang 49. After planting, the seedlings were allowed to establish for 75 days (germination phase to late tillering phase). During this period, seedlings were fertilized, and pest management was carried out by following commercial cultivation practices. Throughout the experiment period, seedlings were watered till the pot capacity to maintain the equal level of soil moisture. To maintain adequate nutrient status of soil, nitrogen (N; 70 mg/kg soil), potassium (P; 50 mg/kg soil) and phosphorous (K; 100 mg/kg soil) were applied to the soil and hogland solution (150 mL/pot) was applied once in two weeks. During the study period, a natural cold front (duration of 6 days) occurred in December 2018 in this region. The daily average temperature was 16.6 °C and 6 °C before and during the cold front, respectively (Fig. 1A). The date of occurrence and duration of the cold front were calculated using the predictions of local forecasts (Nanning, China).

2.2. Foliar application of nanoparticles (NPs)

Seven days before the occurrence of the predicted cold front, NPs of silicon dioxide ($nSiO_2$; 5–15 nm, PCode: 1001011232), zinc oxide (nZnO; < 100 nm, PCode: 1001011300), selenium (nSe; 100 mesh, PCode: 1002171028), graphene (graphene nanoribbons [GNRs] alkyl functionalized; 2–15 μm × 40–250 nm, PCode: 1002232815) (Sigma Aldrich, USA) were sprayed on the leaves of the cultivar Guitang 49. The NPs were prepared by dispersing them in distilled water using mechanical stirrer and 30 min of ultra-sonication for nZnO and nSe, while 3 h of ultra-sonication was given for dissolving $nSiO_2$ and GNRs. Scanning electron microscope (SEM) was used to confirm nanoparticles size using JEOL SEM, JSM.IT100 (Fig. 1). The NPs concentrations prepared and sprayed were 300 ppm for $nSiO_2$ (Ashkavand et al., 2015), 50 ppm for nZnO (Helaly et al., 2014; Subbaiah et al., 2016), 15 ppm for nSe (Zidan and Omar, 2019) and 50 ppm for GNRs (Zhang et al., 2015). At the same time, seedlings were sprayed with distilled water was considered as control for NPs treatments (NPs control).

2.3. Chlorophyll a fluorescence and P700 redox state

Chlorophyll *a* fluorescence and P700 redox state were measured using Dual PAM-100 (Heinz Walz, Effeltrich, Germany). Chlorophyll fluorescence transients (F_o and F_m) and maximum photo-oxidizable P700 (P_m) were determined from fully exposed mature leaves 2 h after sunset (dark adaptation) by applying a saturation pulse of 10,000 μmol m^{-2} s^{-1} for 300 ms. For P_m measurement, a pre-illumination of far-red light was provided, which is essential for the assessment of P700 transients. The maximum photochemical efficiency of PSII (F_v/F_m) was calculated as follows: $F_v/F_m = (F_m - F_o)/F_m$, where: F_o is the minimum fluorescence at dark adapted state; and F_m is the maximum fluorescence at dark-adapted state. The F_v/F_m and P_m was recorded on the 7th day after the application of NPs (before cold front; control) and subsequently from the 3rd day to the 6th day (during cold front). The F_v/F_m and P_m measurements recorded on 5th day after the last day of cold front used to assess the recovery (daily average temperature; 10 °C). The recorded F_v/F_m and P_m from Guitang 49 were compared with Guitang 28 to assess the changes in level of tolerance due to the effect of NPs appliocation.

The other chlorophyll *a* fluorescence and P700 transients were recorded from Guitang 49 on the same days along with gas exchange

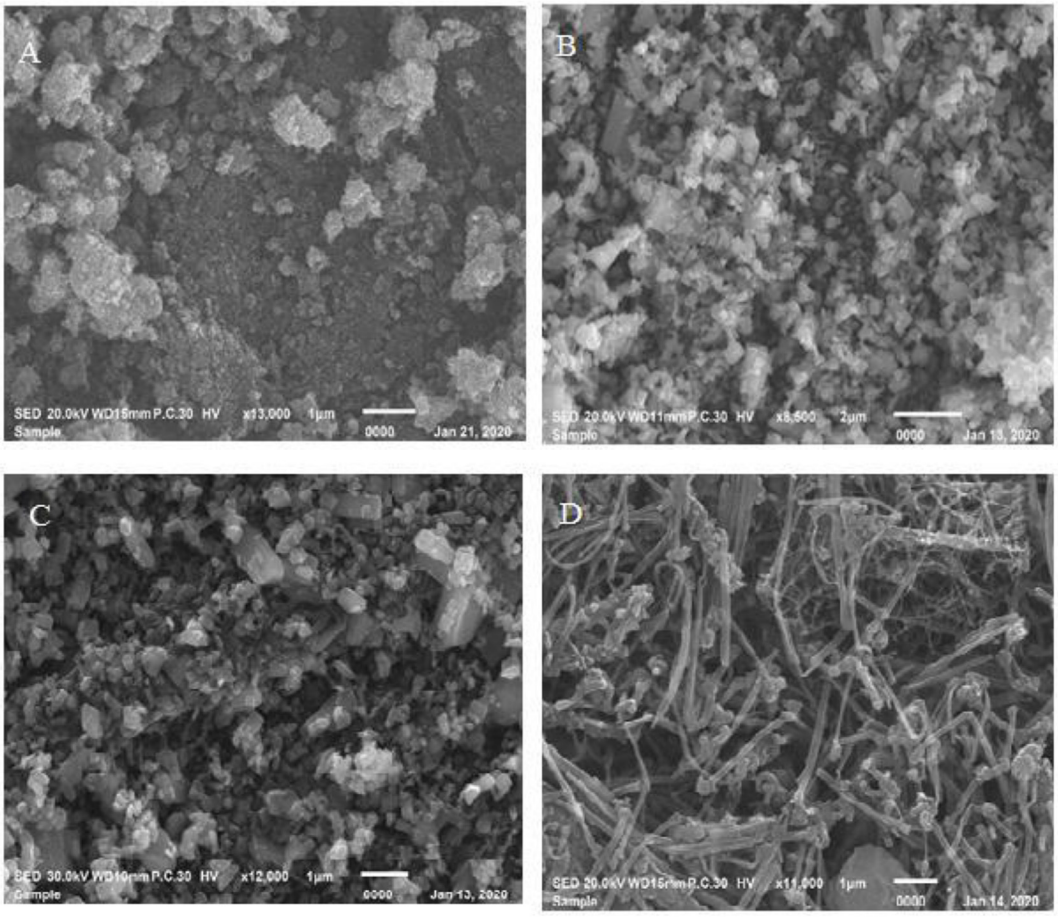

Fig. 1. SEM images of nano SiO2 (A), nano ZnO (B), nano Se (C) and nano GNRs (D).

measurements (7th day after the application of NPs [before cold front; control] and 6th day [during cold front]). Light adapted chlorophyll fluorescence transients were recorded after 30 min of light exposure using artificial lights with a PAR intensity of 500 μmol m^{-2} s^{-1} and applying a saturating pulse of 10,000 μmol m^{-2} s^{-1} for 300 ms. For P700 transients, a pre-illumination of far-red light was provided. Recorded light-adapted chlorophyll fluorescence transients were calculated as follows: Y(II) = $(F_m - F_s)/F_m'$, Y(NPQ) = 1-Y(II) –Y(NO), Y (NO) = F_s/F_m' and qP = $(F_m' - F_o)/(F_m' - F_o')$ (Genty et al., 1989; Oxborough and Baker, 1997; Kramer et al., 2004). Y(II) is the effective photochemical quantum yield of PSII, Y(NO) is the quantum yield of nonregulated energy dissipation, Y(NPQ) is the fraction of energy dissipated as heat through regulated nonphotochemical quenching (NPQ), F_m' is the maximum fluorescence in the light adapted state, F_s is the light adapted steady state fluorescence, F_o' is the minimum fluorescence at light adapted state and qP is a measure of overall reduced and oxidizable PSII centers (Kramer et al., 2004).

The Y(I) is the effective photochemical quantum yield of PSI, which was calculated from Y(ND) and Y(NA) as follows: Y(I) = 1 − Y(ND) − Y (NA). Y(ND) (donor side limitation) is the fraction of overall P700 that is oxidized in a given state and calculated as follows: Y(ND) = 1 − P700 (red). Y(NA) (acceptor side limitation) represents the fraction of overall P700 that cannot be oxidized in a given state due to lack of acceptors and calculated as follows: Y(NA) = $(P_m - P_m')/P_m$. P700 (red) represents the fraction of overall P700 reduced in a given state and P_m' is the maximum photo-oxidizable P700 at the light adapted state (Klughammer and Schreiber, 1994, 2008).

2.4. Photosynthetic electron flow (ETR I and ETR II) and quantum yield of cyclic electron flow Y(CEF)

ETR II and ETR I represent the rate of electron transport of PSII and PSI, respectively and it was calculated using the following formula: ETR II = Y(II) × PAR × 0.5 × *a* and ETR I = Y(I) × PAR × 0.5 × *a*; where *a* is the light absorptance ratio of a leaf and 0.5 is a factor that accounts for the partitioning of light energy between PSII and PSI (Maxwell and Johnson, 2000; Huang et al., 2016a,b). In this experiment, *a* was measured for sugarcane using a miniature leaf spectrometer (CI-710; Camas, WA, USA) and it was 0.75. The effective quantum yield of cyclic electron flow [Y(CEF)] was estimated as: Y (CEF) = Y(I) – Y(II) and LEF was calculated as: LEF = ETR I + ETR II (Miyake et al., 2005; Huang et al., 2010, 2015, 2011; Gao and Wang, 2012).

In this study, Dual PAM-100 instrument was used to measure P700 redox state. The results may not be perfect due to the underestimation of LEF, consequently overestimation of CEF as the Dual PAM-100 measuring chlorophyll *a* fluorescence from leaf mesophyll cells near to the leaf surface and P700 from the signal from whole tissue (Huang et al., 2011). However, Dual PAM 100 is the best commercially available instrument for measuring the P700 redox state because of the ability to simultaneously measure chlorophyll fluorescence and P700. Despite of under and overestimation of LEF and CEF, respectively, earlier researchers and our self believe that relative change in LEF and CEF in response to chilling is reliable to understand the general trend. The methodology for measuring the P700 redox state was firstly reported in Klughammer and Schreiber (1994) and it has been extensively adopted in number of studies on CEF (Miyake et al., 2005; Huang et al. 2010, 2015, 2011; Gao and Wang, 2012).

2.5. Gas exchange and light harvesting pigments

Gas exchange was measured from Guitang 49 on the 7th day after the application of NPs (before cold front; control) and on the 6th day during cold front. Photosynthetic rate (P_N), stomatal conductance (*gs*) and internal CO_2 concentration (C_i) were recorded using a portable photosynthesis system (LI-6800; LICOR, Lincoln, NE, USA) from fully exposed mature leaves. From each NPs treatment and NPs control, a minimum of six measurements were recorded between 0900 and 1100 h. Photosynthetic active radiation (PAR) in the leaf chamber was adjusted to 1000 μmol m^{-2} s^{-1} and ambient CO_2, temperature and relative humidity were used while recording gas exchange. The carboxylation capacity (CE) was calculated from the ratio of P_N to C_i (P_N/C_i) (Rymbai et al., 2014). Foliar chlorophyll *a* (Chl *a*) and *b* (Chl *b*) and carotenoids were measured by following the methods of Welburn (1994).

3. Statistical analysis

For statistical analysis of the data, six biological replications per NPs treatment, NPs control and different temperatures conditions were used for each trait. Analysis of variance (ANOVA) was performed to test the significance of differences among NPs treatments, temperature conditions and their interaction. Spilt plot statistical design was used for current experiment. A generalized linear model (GLM) was in SPSS (SPSS Inc. Ver.16, Chicago, IL, USA) was used for statistically analysing the effects of NPs treatments and different temperature conditions. Means were also compared using post-hoc Duncan's multiple range test (DMRT).

4. Results and discussion

The results of ANOVA revealed the significant effects of different temperature conditions, foliar NPs treatments and in some cases of their interactions in the various physiological traits of the sugarcane variety Guitang 49 (Table 2). NPs enter in to the leaves through cuticular membrane, epidermis and stomata, and travel by different transportation methods (apoplast and symplast). Apoplastic transport is through outside the plasma membrane via extracellular spaces, cell walls of cells and xylem vessels. At the same time, symplastic transport between cells through cytoplasm of adjacent cells through plasmodesmata and sieve plates. The apoplastic pathway is essential for circular transport within plant and permits NPs to get in to the root central cylinder and the vascular tissues for further transport in upward direction (Perez-de-Luque, 2017). Different NPs of different elements used in this study has already proved their role in supporting the plant growth, development

Table 2
Probability values of effect of foliar nanoparticle treatments (NPs), different temperatures conditions (before and during cold front [BUC]) and their interaction (NPs x BUC) on gas exchange, light-energy utilization in PSII, redox state of PSI, cyclic electron flow (CEF) and light harvesting pigments of sugarcane variety (moderately chilling tolerant [Guitang 49]).

Variables			
Traits	Before and during cold front (BUC)	Foliar nanoparticle treatment (NPs)	NPs x BUC
Y(I)	< 0.01	< 0.01	0.578
ETR1	< 0.01	< 0.01	< 0.01
Y(ND)	< 0.01	< 0.01	0.371
Y(NA)	< 0.01	< 0.01	0.163
Y(II)	< 0.01	< 0.01	< 0.05
ETRII	< 0.01	< 0.01	< 0.05
Y(NO)	< 0.01	< 0.01	0.247
Y(NPQ)	< 0.01	< 0.01	0.375
qP	< 0.01	< 0.01	0.672
Y(CEF)	< 0.01	< 0.01	0.468
LEF	< 0.01	< 0.01	< 0.001
F_v/F_m	< 0.01	< 0.01	0.272
P_N	< 0.01	< 0.01	0.697
g_S	< 0.01	< 0.01	0.833
CE	< 0.01	< 0.01	0.093
Chl *a*	< 0.01	< 0.01	< 0.05
Chl *b*	< 0.01	< 0.01	< 0.05
Carotenoids	< 0.01	< 0.01	< 0.05

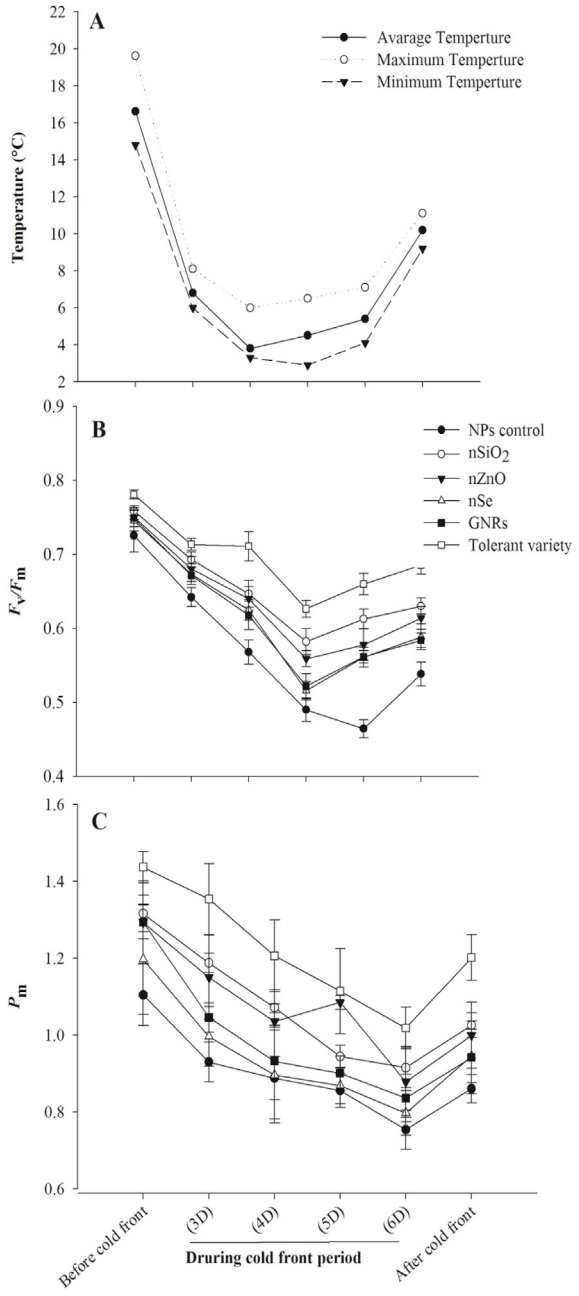

Fig. 2. (A) Atmospheric temperature (average, minimum and maximum) during the period of the experiment at experiment location and (B) maximum photochemical efficiency of PII (F_v/F_m) and (C) maximum photo-oxidizable P700 (P_m) of two sugarcane varieties (moderately chilling tolerant [Guitang 49] and tolerant [Guitang 28]) treated with different foliar nanoparticle treatments (NPs) under different temperature conditions (before and during cold front and recovery).

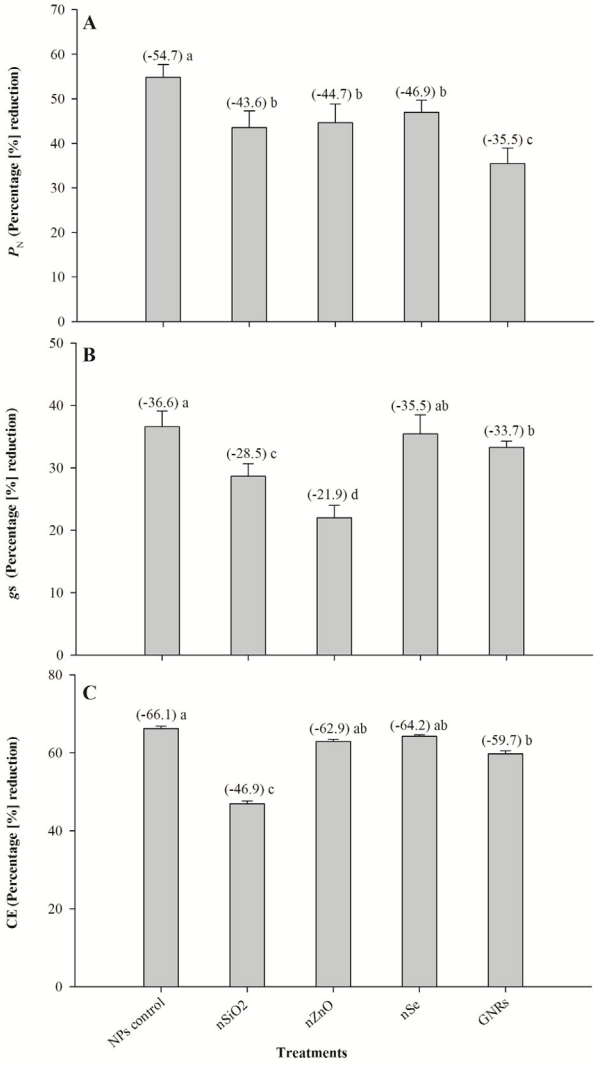

Fig. 3. Percentage decrease in (A) photosynthetic rate (P_N), (B) stomatal conductance (*gs*), and (C) carboxylation capacity (CE) of sugarcane variety (moderately chilling tolerant [Guitang 49]) treated with different foliar nanoparticle treatments (NPs) during cold front (≤10 °C) as compared to before cold front (≥16 °C). The different letters indicate significant differences among the treatments according to Duncan's multiple range test ($P < 0.01$; the test was conducted independently for different temperature conditions).

and protection under optimum and abiotic stress conditions. The major roles of different elements are increased antioxidant capacity (selenium [nSe]; Hasanuzzaman et al., 2010), regulation of potential genes involved in the major physiological and biochemical functions (silicon [$nSiO_2$]; Manivannan and Ahn, 2017), improved chlorophyll index, efficiency of PSII and decreased oxidative stress (zinc [nZnO] Abdel Latef et al., 2016) and biomass production (allotrope of carbon [GNRs] Pandey et al., 2018).

Cold front incidence negatively affected the maximum photochemical efficiency of PSII (F_v/F_m), maximum photo-oxidizable P700 (P_m), and photosynthesis (Figs. 2 and 3). At the same time, during cold front, foliar application of NPs maintained higher F_v/F_m and P_m compared to that of the NPs control (Fig. 2 and Table 3). Before and during the cold front, the chilling tolerant variety Guitang 28 had higher values of F_v/F_m and P_m than the moderately chilling tolerant Guitang 49 of either NPs control and treated with NPs (Fig. 2). The NPs control seedlings of Guitang 49 had lowest values of F_v/F_m and P_m than those treated with NPs. Moreover, the Guitang 49 seedlings sprayed with $nSiO_2$ had higher F_v/F_m and P_m than those treated with other NPs, particularly with nSe and GNRs (Figs. 2 and 4). The F_v/F_m value is an important indicator in plant stress physiology (Mullar et al., 2001; Laxman et al., 2013; Sunoj et al., 2016). Improved F_v/F_m and P_m demonstrates the amelioration capacity of NPs on chilling tolerance in Guitang 49. Previous studies by Singh et al. (2018) and Torabian et al. (2017) have reported that NPs increased fluorescence values in PSII and lower values of energy flux in rice seedlings and sunflower grown under normal and saline condition, respectively. Simultaneously, in Guitang 49, higher P_N, *gs*, and CE values in NPs treated seedlings and positive

Table 3
Effect of foliar nanoparticle treatments (NPs) on gas exchange, light-energy utilization in PSII, redox state of PSI, cyclic electron flow (CEF) and light harvesting pigments of sugarcane variety (moderately chilling tolerant [Guitang 49]) under different temperature conditions (before and during cold front). Values in the parenthesis are ± standard error of respective mean values.

Traits	Before cold front					During cold front				
	NPs Control	$nSiO_2$	nZnO	nSe	GNRs	NPs Control	$nSiO_2$	nZnO	nSe	GNRs
Y(II)	0.113 (± 0.003)	0.151 (± 0.004)	0.131 (± 0.004)	0.120 (± 0.005)	0.148 (± 0.004)	0.039 (± 0.004)	0.057 (± 0.006)	0.052 (± 0.003)	0.043 (± 0.002)	0.041 (± 0.004)
Y(I)	0.216 (± 0.02)	0.298 (± 0.03)	0.274 (± 0.01)	0.258 (± 0.01)	0.263 (± 0.01)	0.159 (± 0.11)	0.254 (± 0.20)	0.238 (± 0.11)	0.202 (± 0.11)	0.179 (± 0.03)
qP	0.153 (± 0.011)	0.264 (± 0.035)	0.210 (± 0.051)	0.220 (± 0.041)	0.188 (± 0.033)	0.089 (± 0.010)	0.179 (± 0.008)	0.159 (± 0.017)	0.137 (± 0.022)	0.113 (± 0.017)
Y(NPQ)	0.390 (± 0.03)	0.479 (± 0.09)	0.443 (± 0.03)	0.433 (± 0.03)	0.432 (± 0.07)	0.411 (± 0.02)	0.538 (± 0.03)	0.492 (± 0.05)	0.465 (± 0.01)	0.477 (± 0.02)
Y(NO)	0.498 (± 0.03)	0.370 (± 0.09)	0.445 (± 0.02)	0.447 (± 0.03)	0.420 (± 0.07)	0.551 (± 0.02)	0.405 (± 0.03)	0.456 (± 0.04)	0.492 (± 0.01)	0.482 (± 0.02)
LEF	88 (± 1.9)	131 (± 2.3)	118.1 (± 2.3)	109.7 (± 5.0)	98.4 (± 4.4)	53.1 (± 4.9)	77.4 (± 3.7)	71.5 (± 3.2)	66.6 (± 1.7)	66 (± 2.2)
Y(CEF)	0.103 (± 0.015)	0.147 (± 0.035)	0.142 (± 0.008)	0.138 (± 0.003)	0.116 (± 0.014)	0.121 (± 0.007)	0.197 (± 0.031)	0.185 (± 0.014)	0.158 (± 0.003)	0.136 (± 0.049)
Y(ND)	0.704 (± 0.016)	0.650 (± 0.029)	0.662 (± 0.010)	0.675 (± 0.012)	0.665 (± 0.017)	0.785 (± 0.029)	0.716 (± 0.019)	0.728 (± 0.006)	0.759 (± 0.008)	0.770 (± 0.030)
Y(NA)	0.081 (± 0.003)	0.052 (± 0.002)	0.065 (± 0.003)	0.067 (± 0.005)	0.072 (± 0.005)	0.056 (± 0.003)	0.031 (± 0.006)	0.034 (± 0.006)	0.040 (± 0.006)	0.051 (± 0.003)
ETR I	59.8 (± 2.9)	89.1 (± 3.8)	78.5 (± 3.8)	77.4 (± 2.9)	67.2 (± 2.7)	34.1 (± 2.6)	50.3 (± 2.3)	46.3 (± 2.0)	43.3 (± 1.7)	43.2 (± 3.1)
ETR II	28.2 (± 1.3)	41.9 (± 3.0)	39.6 (± 2.0)	32.3 (± 2.1)	31.2 (± 1.7)	19 (± 2.5)	27.1 (± 2.0)	25.1 (± 1.3)	23.3 (± 0.7)	22.8 (± 1.5)
P_N	14.953 (± 0.49)	20.901 (± 0.29)	20.416 (± 0.48)	18.773 (± 0.89)	17.039 (± 1.08)	6.759 (± 0.62)	11.794 ± (0.68)	11.299 (± 0.58)	9.952 (± 0.41)	10.992 (± 0.75)
g_S	0.108 (± 0.007)	0.133 (± 0.005)	0.122 (± 0.006)	0.110 (± 0.012)	0.112 (± 0.010)	0.068 (± 0.012)	0.095 (± 0.014)	0.095 (± 0.005)	0.071 (± 0.012)	0.074 (± 0.005)
CE	0.077 (± 0.006)	0.106 (± 0.011)	0.135 (± 0.006)	0.107 (± 0.007)	0.103 (± 0.007)	0.026 (± 0.002)	0.056 (± 0.003)	0.050 (± 0.003)	0.038 (± 0.003)	0.042 (± 0.002)
F_v/F_m	0.73 (± 0.02)	0.76 (± 0.007)	0.75 (± 0.013)	0.75 (± 0.014)	0.75 (± 0.012)	0.54 (± 0.016)	0.63 (± 0.011)	0.61 (± 0.015)	0.59 (± 0.017)	0.58 (± 0.009)
P_m	1.10 (± 0.08)	1.32 (± 0.047)	1.29 (± 0.11)	1.20 (± 0.14)	1.29 (± 0.044)	0.75 (± 0.051)	0.91 (± 0.052)	0.88 (± 0.092)	0.80 (± 0.058)	0.84 (± 0.06)
Chl *a*	8.19 (± 0.17)	10.2367 (± 0.16)	9.5333 (± 0.27)	8.61 (± 0.28)	8.02 (± 0.18)	5.02 (± 0.16)	6.41 (± 0.21)	6.34 (± 0.18)	5.53 (± 0.37)	5.01 (± 0.3)
Chl *b*	4.05 (± 0.10)	4.89 (± 0.12)	4.43 (± 0.12)	4.28 (± 0.15)	3.97 (± 0.153)	2.18 (± 0.13)	3.15 (± 0.1)	2.87 (± 0.152)	2.83 (± 0.14)	2.44 (± 0.12)
Carotenoids	2.52 (± 0.07)	3.48 (± 0.06)	3.12 (± 0.062)	2.68 (± 0.11)	2.74 (± 0.09)	4.32 (± 0.06)	6.11 (± 0.08)	5.67 (± 0.07)	5.12 (± 0.11)	5.02 (± 0.11)

correlations of these parameters with F_v/F_m further support the efficiency of these NPs treatments to protect the seedlings from chilling (Figs. 3 and 5).

Recently, many researchers have reported that NPs improve P_N and photoprotection, which results in higher crop yield under various a biotic stress conditions. For instance, improved crop yield in sorghum under drought stress with the application of NPs was reported by Djanaguiraman et al. (2018). Similarly, Siddique et al. (2014) and Shi et al. (2013) found that $nSiO_2$ application increased P_N under salinity stress in cucumbers and rice. On the other hand, Aghdam et al. (2015) found that NPs of manganese (nMn) treatment improved the photophosphorylation activity of the electron transport chain in the thylakoid membranes of chloroplasts and the P_N in flax. Moreover, Qi et al. (2013) reported that NPs of titanium oxide ($nTiO_2$) treatment increased P_N by regulating energy dissipation, which induced cooling of leaves through prompt stomatal opening in tomato. The higher P_N is associated with increase of the stomatal opening in soybean with foliar applications of NPs of ferric oxide (nFe_2O_3) (Alidoust and Isoda, 2013). In the present study, NPs treated seedlings showed higher P_N than that of the control. At the same time, among the NPs treatments, sugarcane seedlings treated with $nSiO_2$ showed a higher rate of P_N followed by nZnO, GNRs, and nSe treatments under both temperature conditions (Fig. 3). Concurrently, the same trend was observed in *gs* and CE with these treatments.

Furthermore, before cold front, foliar application of NPs increased the chl *a* and *b* contents in sugarcane leaves and the rate of increase was higher in $nSiO_2$ treatment followed by nZnO, nSe, and GNRs treatments as compared to that of NPs control plants (Fig. 6). Previous studies have reported that foliar application of NPs significantly increase the chlorophyll content in plants, which reveals that NPs supported plants to synthesize additional light harvesting complexes to capture large amounts of light energy, leading to increased P_N (Kuang, 2003; Hong et al., 2005; Ghafariyan et al., 2013). Meanwhile, during cold front, chl *a* and *b* contents were significantly reduced, while the rate of reduction was lower in seedlings treated with NPs than that of the control, which helped to maintain the P_N in sugarcane seedlings.

In contrast to the response of chlorophyll content, carotenoids were increased during cold front (Fig. 6). The highest rate of increase in carotenoids was in the $nSiO_2$ treatment followed by the nZnO, nSe, and GNRs treatments. Oxygen containing carotenoids (xanthophylls) are involved in the non-photochemical quenching (NPQ; qN) of excess energy on PSII via the xanthophyll cycle, which is important to prevent photoinhibition or photodamage to the photosystems and maintain the P_N (Muller et al., 2001; Derks et al., 2015). Changes in the light harvesting pigments in response to NPs have been reported in previous studies (Ghafariyan et al., 2013: Rad et al., 2014; Falco et al., 2015; Torabian et al., 2017). Higher carotenoid contents after application of NPs improved the photoprotection and thereby the P_N in sugarcane

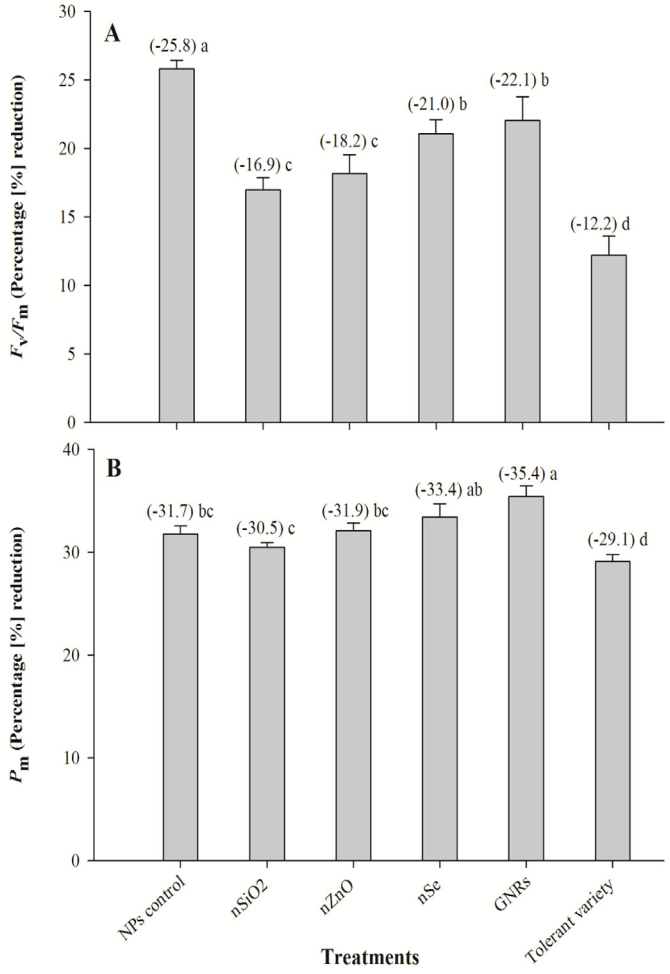

Fig. 4. Percentage decrease in (A) Maximum quantum yield of PSII (F_v/F_m) and (B) P_m: maximum photo-oxidizable PSI of sugarcane variety (moderately chilling tolerant [Guitang 49]) treated with different foliar nanoparticle treatments (NPs) during cold front (≤10 °C) as compared to before cold front (≥16 °C). The different letters indicate significant differences among the treatments according to Duncan's multiple range test ($P < 0.01$; the test was conducted independently for different temperature conditions).

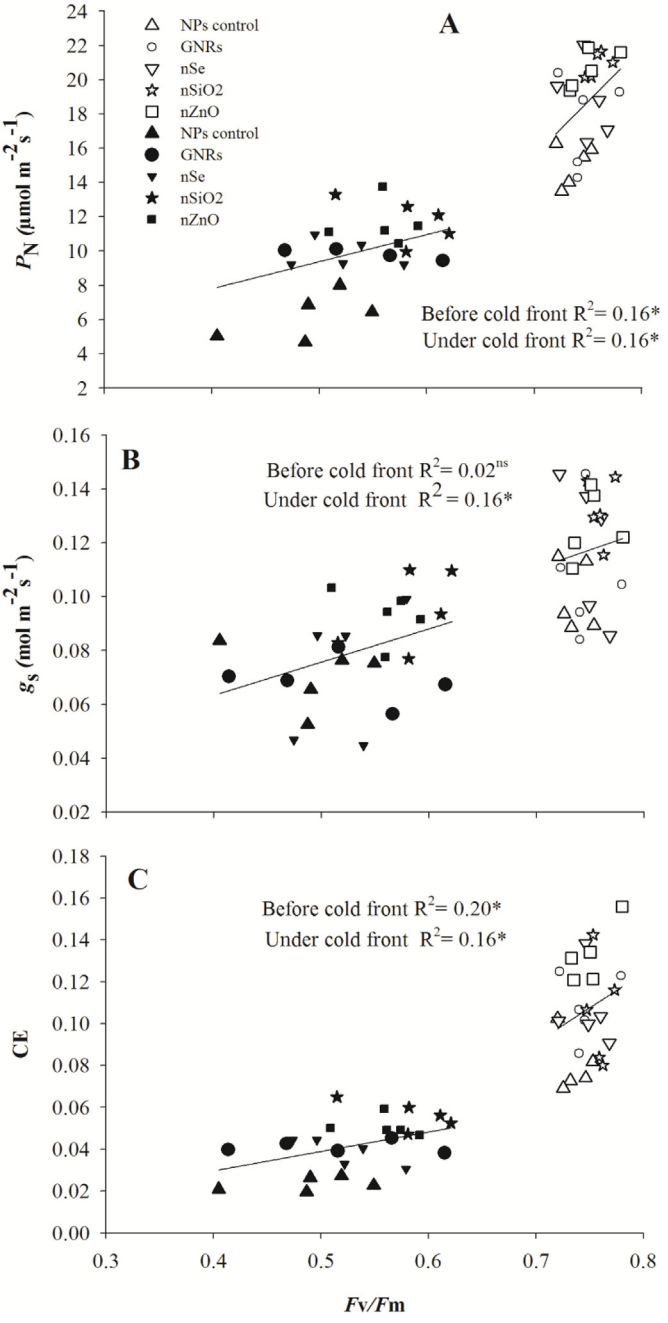

Fig. 5. Relationship of maximum photochemical efficiency of PII (F_v/F_m) with (A) photosynthesis rate (P_N), (B) stomatal conductance (gs) and (C) carboxylation capacity (CE) of sugarcane variety (moderately chilling tolerant [Guitang 49]) treated with different foliar nanoparticle treatments (NPs) under different temperature conditions (before [≥16 °C; white symbols] and during cold front [≤10 °C; black symbols]). Coefficient of determination (R^2) followed by ns, * and ** correspond to non-significant, significance at $P < 0.05$ and $P < 0.01$, respectively.

seedlings during cold front.

The Y(NPQ) was higher during cold front than before cold front, while the increment rate was higher in NPs treatments than in the NPs control (Fig. 7 and Table 3). The Y(NPQ) is the portion of energy dissipated as heat through the photoprotective Y(NPQ) mechanism (Klughammer and Schreiber, 2008). On the other hand, qP was reduced during cold front but maintained in the seedlings treated with NPs. (Fig. 7 and Table 3). The qP is a measure of overall reduced and oxidizable PSII centers. The qP values vary between 1 (defined for dark adapted state) to 0 (PS II centers all closed) and Y(NO) is the quantum yield of nonregulated energy dissipation (Kramer et al., 2004). Lower Y (NO) values after NPs applications indicate that both photochemical energy conversion and protective regulatory mechanisms were efficient to prevent photoinhibition in PSII (Kramer et al., 2004; Klughammer and Schreiber, 2008). The $nSiO_2$ treatment showed higher Y(NPQ) and qP and lower Y(NO) than other NPs treatments (Fig. 7 and Table 3), which indicates that the $nSiO_2$ treatment increased the efficiency to manage excess energy, maintained the electron load, avoided photoinhibition, and maintained the P_N and CE. These changes can help maintain sustainable growth after cold front.

The ability of NPs treatments to maintain P_N and CE were further evident from enhanced photochemical yield of photosystem reaction centers (PS I [Y(I)] and PSII [Y(II)]) and electron flow (PSII [ETR (II)] and PSI [ETR (I)]) between the photosystems (LEF) compared to that of the NPs control (Table 3). During cold front, there was a reduction in Y (I) and Y(II) (Fig. 8 and Table 3), but the reduction was lower in seedlings treated with NPs and among the NPs, reduction was least in $nSiO_2$ treatment, followed by nZnO, nSe and GNRs treatments. The same trend was observed in the electron transport rate of PSII [ETR (II)], PSI [ETR (I)] and linear electron flow (LEF) (Table 3). Whereas,

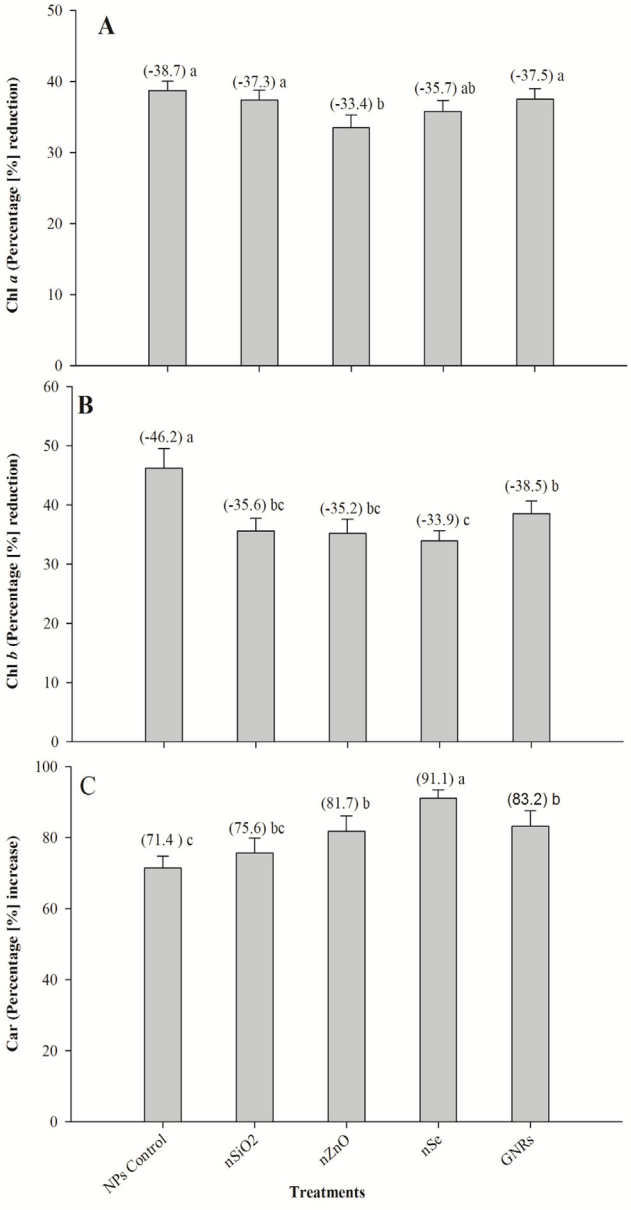

Fig. 6. Percentage change in (A) Chlorophyll *a* (Chl *a*), (B) Chlorophyll *b* (Chl *b*), and (C) carotenoids (Car) of sugarcane variety (moderately chilling tolerant [Guitang 49]) treated with different foliar nanoparticle treatments (NPs) during cold front (≤10 °C) as compared to before cold front (≥16 °C). The different letters indicate significant differences among the treatments according to Duncan's multiple range test ($P < 0.01$; the test was conducted independently for different temperature conditions).

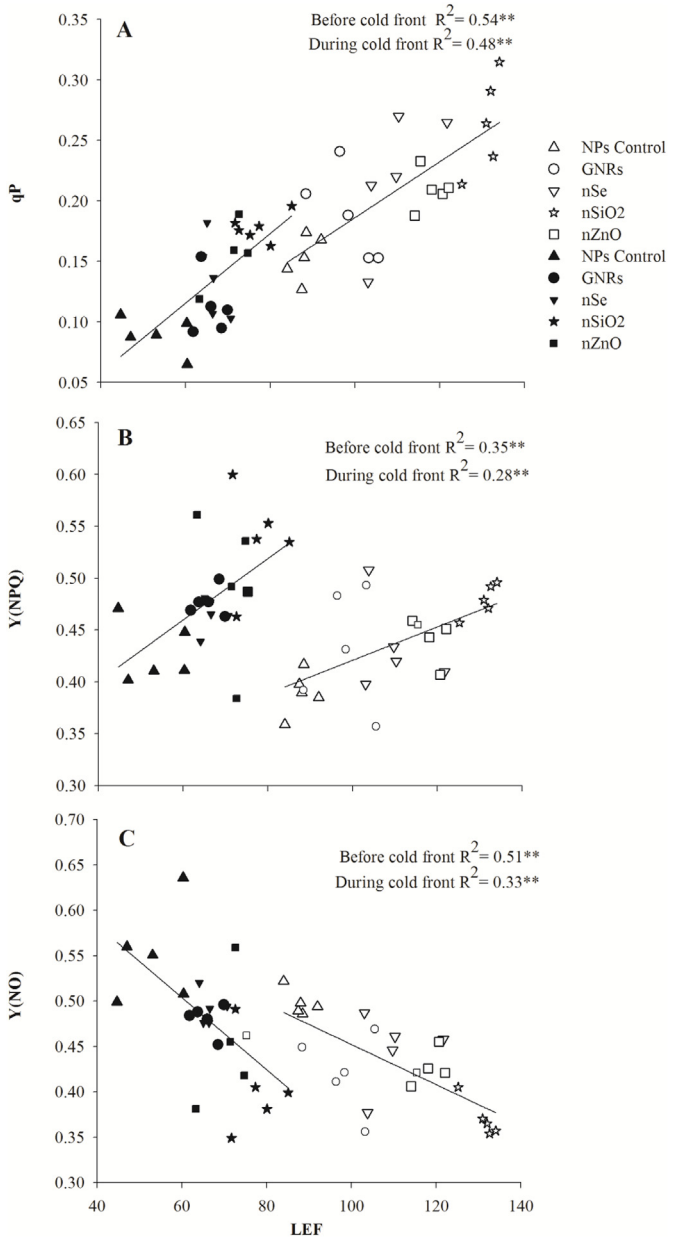

Fig. 7. Relationship of linear electron flow (LEF) with (A) Coefficient of photochemical quenching (qP), (B) yield of regulated energy dissipation Y(NPQ), and (C) yield of non-regulated energy dissipation Y(NO) of sugarcane variety (moderately chilling tolerant [Guitang 49]) treated with different foliar nanoparticle treatments (NPs) under different temperature conditions (before [≥16 °C; white symbols] and during cold front [≤10 °C; black symbols]). Coefficient of determination (R^2) followed by * and ** correspond to significance at $P < 0.05$ and $P < 0.01$, respectively.

the effective quantum yield of cyclic electron flow Y(CEF) was enhanced in the seedlings during cold front and treated with NPs (Fig. 9).

Meanwhile, during cold front, $nSiO_2$ treatment exhibited higher Y (CEF) than that of the nZnO treatment (Fig. 9 and Table 3). Activation of Y(CEF) is important when photoinhibition accelerates and CO_2 fixation is limited (Takahashi et al., 2009; Agrawal et al., 2016; Neto et al., 2017). There are a few main functions of Y(CEF) that tend to mitigate the hazardous impact of various stresses, thereby severe damage of PSII is prevented and ultimately PSI is protected. Y(CEF) activates Y(NPQ) by generating a higher proton gradient (ΔpH) between the thylakoid lumen and stoma (Mohanty et al., 2007; Allakhverdiev, 2011; Joliot and Johnson, 2011; Sonoike, 2011; Kono and Terashima, 2016; Huang et al., 2018).

During cold front, activation of Y(CEF) and higher F_v/F_m and P_m in the NPs treated sugarcane seedlings proved an important role of NPs to enhance Y(NPQ), which helped to mitigate photoinhibition. This is evident by the positive correlation of LEF with Y(II), Y(I), Y(NPQ), qP, and Y(CEF) and the negative correlation with Y(NO), Y(ND), and Y(NA) (Figs. 7–9). Application of NPs reduced Y(ND) and Y(NA) in seedlings before and during cold front, which are associated with the higher P_N and efficient energy management of photosystems, as shown here. Y (ND) is a measure of donor side limitation of PSI, which is enhanced by the proton gradient across the thylakoid membranes and damage of PSII reaction centers. Lower Y(ND) value in NPs treated seedlings indicate the unclogged LEF between photosystems and least damage to PSII.

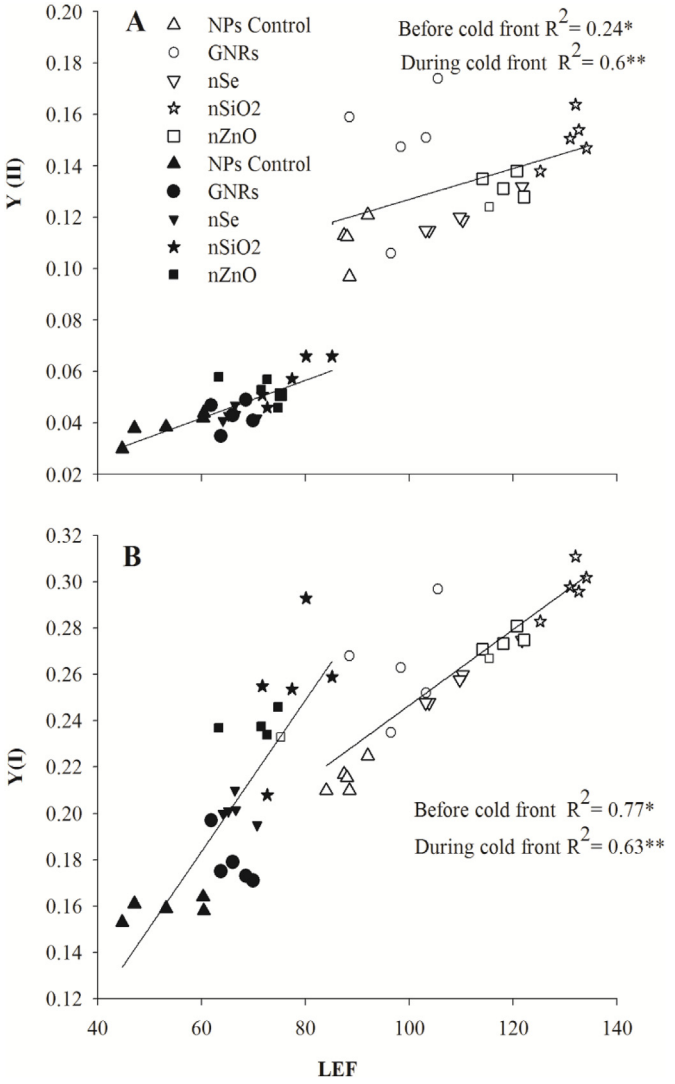

Fig. 8. Relationship of linear electron flow (LEF) with (A) effective photochemical quantum yield of PSII [Y(II)], and (B) effective photochemical quantum yield of PSI [Y(I)] of sugarcane variety (moderately chilling tolerant [Guitang 49]) treated with different foliar nanoparticle treatments (NPs) under different temperature conditions (before [≥16 °C; white symbols] and during cold front [≤10 °C; black symbols]). Coefficient of determination (R^2) followed by * and ** correspond to significance at $P < 0.05$ and $P < 0.01$, respectively.

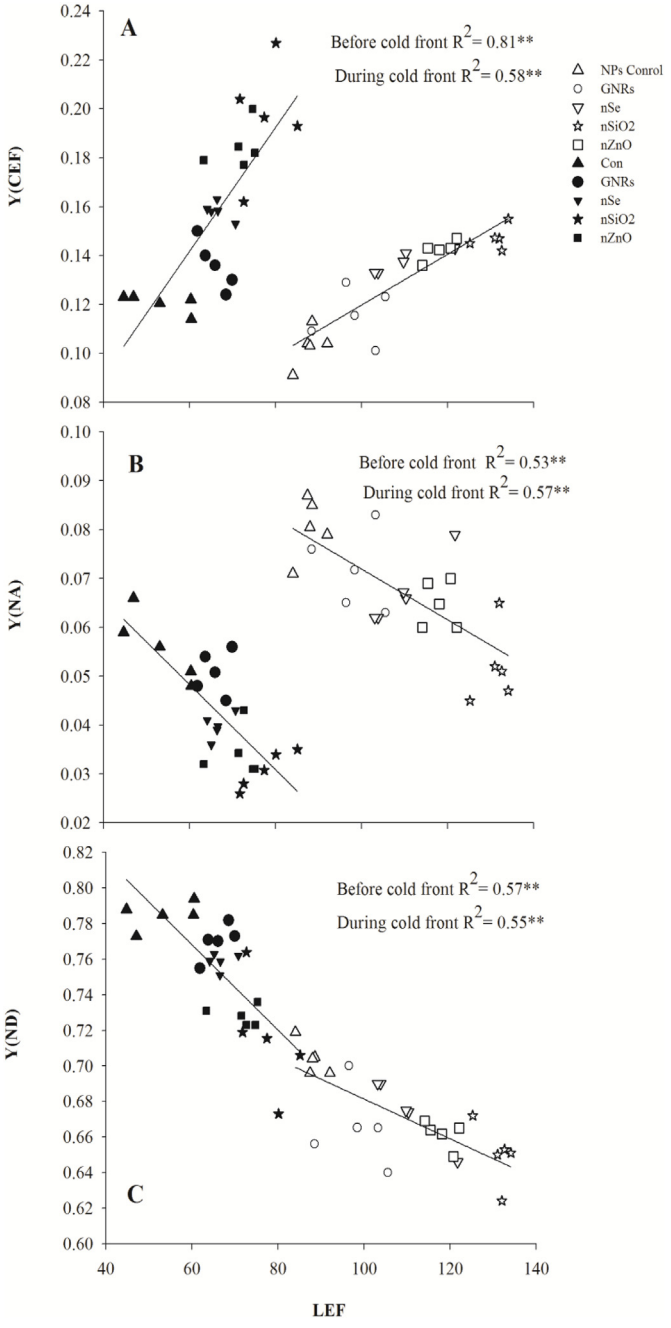

Fig. 9. Relationship of linear electron flow (LEF) with (A) effective quantum yield of CEF (Y[CEF]), (B) PSI donor side limitation (Y(ND]), and (C) PSI acceptor side limitation (Y[ND]) of sugarcane variety (moderately chilling tolerant [Guitang 49]) treated with different foliar nanoparticle treatments (NPs) under different temperature conditions (before [≥16 °C; white symbols] and during cold front [≤10 °C; black symbols]). Coefficient of determination (R^2) followed by * and ** correspond to significance at $P < 0.05$ and $P < 0.01$, respectively.

Meanwhile, Concurrently, Y(NA) is the ratio of reduced and oxidized acceptor side of PSI (acceptor side limitation), and lower Y(NA) values imply that active dark reaction of photosynthesis (Kono and Terashima, 2016). Among the different NPs treatments, $nSiO_2$ treatment exhibited the highest reduction of Y(ND) and Y(NA) in both temperature conditions.

5. Conclusions

The results of the current study clearly demonstrated the capacity of different NPs to ameliorate the tolerance to chilling. Among NPs treatments, the $nSiO_2$ treatment showed promising results by enhancing photosynthesis and improving photoprotection. The capability of NPs to maintain the chlorophyll content and increase the carotenoid content helped to increase the NPQ in NPs treated seedlings, which was initiated by the activation of Y(CEF) and the triggering point for the cascade of other photoprotection mechanisms. The present study demonstrates that individual NPs or a consortium of NPs can be applied to mitigate the negative impact of chilling stress in sugarcane.

Author's contribution

Nabil I elsheery and Cao KunFang designed research. NIE, VSJS, YW, and GM conducted the experiment and collected the data. NIE and VSJS contributed to the analysis of the data and statistics. JJZ provided sugarcane verities for the research. KFC supervised the research, suggested critical comments and corrections while preparing manuscript. All the authors contributed for the final version of the manuscript

Declaration of competing interest

The authors declare that they have no competing interests.

Acknowledgements

This research work was supported by the visiting scholarship (Asian Talented Young Scientist Guangxi Program, China) from Department of Science and Technology, Guangxi Zhuang Autonomous Region, China granted to NIE, also by the postdoctoral fellowship from Guangxi University granted to VSJS and by the Bagui Scholarship (C33600992001) granted to KFC.

References

Abdel-Haliem, M.E., Hegazy, H.S., Hassan, N.S., Naguib, D.M., 2017. Effect of silica ions and nano silica on rice plants under salinity stress. Ecol. Eng. 99, 282–289.

Abdel Latef, A., Alhmad, M., Abdelfattah, K., 2016. The possible roles of priming with ZnO nanoparticles in mitigation of salinity stress in Lupine (*Lupinus termis*) Plants. J. Plant Growth Regul. 36 (1), 60–70.

Aghdam, M.T.B., Mohammadi, H., Ghorbanpour, M., 2015. Effects of nanoparticulate anatase titanium dioxideon physiological and biochemical performance of *Linumu sitatissimum* (Linaceae) under well-watered anddrought stress conditions. Braz. J. Bot. 39 (1), 139–146.

Agrawal, D., Allakhverdiev, S.I., Jajoo, A., 2016. Cyclic electron flow plays an important role in protection of spinach leaves under high temperature stress. Russ. J. Plant Physiol. 63 (2), 210–215.

Alidoust, D., Isoda, A., 2013. Effect of γFe_2O_3 nanoparticles on photosynthetic characteristic of soybean (*Glycine max* (L.) Merr.): foliar spray versus soil amendment. Acta Physiol. Plant. 3365.

Allakhverdiev, S.I., 2011. Recent progress in the studies of structure and function of photosystem II. J. Photochem. Photobiol. B Biol. 104, 1–8.

Allen, D.J., Ort, D.R., 2001. Impacts of chilling temperatures on photosynthesis in warm-climate plants. Trends Plant Sci. 6 (1), 36–42.

Ashkavand, P., Tabari, M., Zarafshar, M., Tomaskova, I., Struve, D., 2015. Effect of SiO_2 nanoparticles on drought resistance in hawthorn seedlings. Lesne Prace Badawcze/ Forest Research Papers 76, 350–359.

Azimi, R., Borzelabad, M., Feizi, H., Azimi, A., 2014. Interaction of sio nanoparticles with seed prechilling on germination and early seedling growth of tall wheatgrass (*Agropyron elongatum* l.). Polish J chem techn 16 (3), 25–29.

Burklew, C.E., Ashlock, J., Winfrey, W.B., Zhang, B., 2012. Effects of aluminium oxide nanoparticles on the growth, development,and microRNA expression of tobacco (*Nicotiana tabacum*). PloS One 7, 34783.

Burman, U., Saini, M., Kuma, P., 2013. Effect of zinc oxide nanoparticles on growth and antioxidant system of chickpea seedlings. Toxicol. Environ. Chem. 95 (4), 605–612.

Cao, K.F., Guo, Y.H., Cai, Z.Q., 2006. Photosynthesis and antioxidant enzyme activity in breadfruit, jackfruit and mangosteen in Southern Yunnan, China. J. Hortic. Sci. Biotechnol. 81 (1), 168–172.

Derks, A., Schaven, K., Bruce, D., 2015. Diverse mechanisms for photoprotection in photosynthesis. Dynamic regulation of photosystem II excitation in response to rapid environmental change. Biochim. Biophys. Acta 1847, 468–485.

Dhillon, R.S., von Wuehlisch, G., 2013. Mitigation of global warming through renewable biomass. Biomass Bioenergy 48, 75–89.

Djanaguiraman, M., Nair, R., Giraldo, J.P., Prasad, V., 2018. Cerium oxide nanoparticles decrease drought-induced oxidative damage in sorghum leading to higher photosynthesis and grain yield. ACS Omega 3, 14406–14416.

Ebrahim, M., Zingsheim, O., El-Shourbagy, M., Moore, P., Komor, E., 1998. Growth and sugar storage in sugarcane grown at temperatures below and above optimum. J. Plant Physiol. 153 (5–6), 593–602.

El-Ramady, H., Abdalla, N., Taha, H., Alshaal, T., El-Henawy, A., Faizy, S., Shams, M., Youssef, S., Shalaby, T., Bayoumi, Y., Elhawat, N., Shehata, S., Sztrik, A., Prokisch, J., Domokos-Szabolcsy, M., Pilon-Smits, E., Selmar, D., Haneklaus, S., Schnug, E., 2015. Selenium and nano-selenium in plant nutrition. Environ. Chem. Lett. 14 (1), 123–147.

Elsheery, N., Wilske, B., Zhang, J.L., Cao, K.F., 2007. Seasonal variations in gas exchange and chlorophyll fluorescence in the leaves of five mango cultivars in southern Yunnan, China. J. Hortic. Sci. Biotechnol. 82 (6), 855–862.

Elsheery, N.I., Wilske, B., Cao, K.F., 2008. The effect of night chilling on gas exchange and chlorophyll fluorescence of two mango cultivars growing under two irradiances. Acta Bot. Yunnanica 30 (4), 447–456.

Factfish, 2015. Sugar cane, production quantity (tons)—for all countries. http://www.factfish.com/statistic/sugar+cane,+production+quantit.

Falco, W.F., Queiroz, A.M., Fernandes, J., Botero, E.R., Falcão, E.A., Guimarães, F.E.G., et al., 2015. Interaction between chlorophyll and silver nanoparticles: a close analysis of chlorophyll fluorescence quenching. J. Photochem. Photobiol. Chem. 299, 203–209.

FAO, 2017. "Report, Food and Agricultural Organization, United Nations: Economic and Social Department," the Statistical Division, FAO 2017. FAOSTAT 2018. http://faostat3.fao.org/home/index.html#DOWNLOAD.

Gao, S., Wang, G.C., 2012. The enhancement of cyclic electron flow around photosystem I improves the recovery of severely desiccated Porphyra yezoensis (Bangiales, Rhodophyta). J. Exp. Bot. 63, 4349–4358.

Genty, B., Briantais, J.M., Baker, N.R., 1989. The relationship between the quantum yield of photosynthetic electron-transport and quenching of chlorophyll fluorescence. Biochem Biophys Acta 990, 87–92.

Ghafariyan, M.H., Malakouti, M.J., Dadpour, M.R., Stroeve, P., Mahmoudi, M., 2013. Effects of magnetite nanoparticles on soybean chlorophyll. Environ. Sci. Technol. 47 (18), 10645–10652.

Gui, X., Deng, Y., Rui, Y., Gao, B., Luo, W., Chen, S., Nhan, L.V., Li, X., Liu, S., Han, Y., Liu, L., Xing, B., 2015. Response difference of transgenic and conventional rice (*Oryza sativa*) to nanoparticles (γFe2O3). Environ. Sci. Pollut. Res. 22, 17716–17723.

Guo, K., Hu, A., Wang, K., Wang, L., Fu, D., Hao, Y., Wang, Y., Ali, A., Adeel, M., Rui, Y., Tan, W., 2019. Effects of spraying nano-materials on the absorption of metal(loid)s in cucumber. IET Nanobiotechnol. 13 (7), 712–719.

Haghighi, M., Abolghasemia, R., Jaime, A., Teixeira, S., 2014. Low and high temperature stress affect the growth characteristics of tomato in hydroponic culture with Se and nano-Se amendment. Sci Horti 178, 231–240.

Hasanuzzaman, M., Hossain, M.A., Fujita, M., 2010. Selenium in higher plants: physiological role, antioxidant metabolism and abiotic stress tolerance. J. Plant Sci. 5 (4), 354–375.

Helaly, M.N., El-Metwally, M.A., El-Hoseiny, H., Omar, S.A., El-Sheery, N.A., 2014. Effect of nanoparticles on biological contamination of *in vitro* cultures and organogenic regeneration of banana. AJCS 8 (4), 612–624.

Hong, F.S., Yang, F., Ma, Z.N., Zhou, J., Liu, C., Wu, C., Yang, P., 2005. Influences of nano-TiO2 on the chloroplast ageing of spinach under light. Biol. Trace Elem. Res. 104, 249–260.

Hong, L., Li, H., 2001. An investigation reports on the 1999/2000 winter chilling injury to tropical crops in the tropical region of Yunnan Province. Bull Yunnan Crop Sci Technol 2001 (Suppl. ment), 1–9 (in Chinese).

Huang, W., Zhang, S.B., Cao, K.F., 2010. Stimulation of cyclic electron flow during recovery after chilling-induced photoinhibition of PSII. Plant Cell Physiol. 51 (11), 1922–1928.

Huang, W., Zhang, S.B., Cao, K.F., 2011. Cyclic electron flow plays an important role in photoprotection of tropical trees illuminated at temporal chilling temperature. Plant Cell Physiol. 52 (2), 297–305.

Huang, W., Hu, H., Zhang, S., 2016a. Photosynthesis and photosynthetic electron flow in the alpine evergreen species *Quercus guyavifolia* in winter. Front. Plant Sci. 7 Article 1511.

Huang, W., Yang, Y., Hu, H., Cao, K.F., Zhang, S., 2016b. Sustained diurnal stimulation of cyclic electron flow in two tropical tree species *Erythrophleum guineense* and *Khaya ivorensis*. Front. Plant Sci. 7 Article 1068.

Huang, W., Quan, X., Zhang, S.B., Liu, T., 2018. In vivo regulation of proton motive force during photosynthetic induction. Environ. Exp. Bot. 148, 109–116.

Huang, W., Zhang, S.B., Zhang, J., Hu, H., 2015. Photoinhibition of photosystem I under high light in the shade-established tropical tree species *Psychotria rubra*. Front. Plant Sci. 6, 801. https://doi.org/10.3389/fpls.2015.00801.

Hussein, M.M., Abou-Baker, N.H., 2018. The contribution of nano-zinc to alleviate salinity stress on cotton plants. Water Relations and Field Irrigation Department, and Soils and Water Use. Rev. Soc. Sci. 5 (8), 171809.

IPCC, 2013. Summary for policymakers. In: Stocker, T.F., Qin, D., Plattner, G.K., Melinda, M.B.T., Simon, K.A., Judith, B., Alexander, N., Yu, X., Vincent, B., Paulin, M.M. (Eds.), Climate Change: the Physical Science Basis. Contribution of Working Group I to the Fifth Assessment Report of the Intergovernmental Panel on Climate Change. Cambridge University Press, Cambridge, United Kingdom and New York, USA, pp. 1–27.

Joliot, P., Johnson, G., 2011. Regulation of cyclic and linear electron flow in higher plants. Proc. Natl. Acad. Sci. Unit. States Am. 108 (32), 13317–13322.

Karimi, J., Mohsenzadeh S, S., 2016. Effects of silicon oxide nanoparticles on growth and physiology of wheat seedlings. Russ. J. Plant Physiol. 63 (1), 119–123.

Kim, S., Lee, S., Lee, I., 2012. Alteration of phytotoxicity and oxidant stress potential by metal oxide Nnanoparticles in Cucumis sativus. Water, Air, Soil Pollut. 223, 2799–2806.

Klughammer, C., Schreiber, U., 1994. An improved method, using saturating light pulses, for the determination of photosystem-I quantum yield via P700 + -absorbance changes at 830 nm. Planta 192, 261–268.

Klughammer, C., Schreibe, U., 2008. Complementary PS II quantum yields calculated from simple fluorescence parameters measured by PAM fluorometry and the Saturation Pulse method. PAM Application Notes 1, 27–35.

Kono, M., Terashima, I., 2016. Elucidation of photoprotective mechanisms of PSI against fluctuating light photoinhibition. Plant Cell Physiol. 57 (7), 1405–1414.

Kramer, D.M., Johnson, G., Kiirats, O., Edwards, G.E., 2004. New fluorescence parameters for the determination of Q A redox state and excitation energy fluxes. Photosynth. Res. 79, 209–218.

Kuang, T.Y. (Ed.), 2003. Mechanism and Regulation of Primary Energy Conversion Process in Photosynthesis. Science and Technology Press of Jiangsu, Nanjing, pp. 22–68.

Laxman, R.H., Srinivasa, R.N.K., Bhatt, R.M., Sadashiva, A.T., Sunoj, J.V.S., Geeta, B., Pavithra, C.B., Manasa, K.M., Dhanyalakshmi, K.H., 2013. Response of tomato (*Lycopersicon esculentum* Mill:) genotypes to elevated temperature. J. Agrometeorol 15, 38–44.

Li, Y.R., Wu, J.M., Li, X., Zhang, H., Liu, X.H.L.T., 2015. Damage in sugarcane production caused by long duration of chilling frost in Guangxi, China. Inter J Agri Innov Res 3 (4), 1139–1144.

Li, Y.R., Yang, L.T., 2015. Sugarcane industry in China. Sugar Tech 17 (1), 1–8.

Li, Z., Huang, J., 2014. Effects of nanoparticle hydroxyapatite on growth and antioxidant system in pakochoi (Brassica chinensis L.) from cadmium-contaminated soil. J Nanomat 1–7.

Lobell, D.B., Burke, M.B., Tebaldi, C., Mastrandrea, M.D., Falcon, W.P., Naylor, R.L., 2008. Prioritizing climate change adaptation needs for food security in 2030. Science 319 (5863), 607–610.
Ma, X., Geiser-Lee, J., DengY, Kolmakov A., 2010. Interactions between engineered nanoparticles (ENPs)and plants:phytotoxicity, uptake and accumulation. Sci. Total Environ. 408, 3053–3061.
Mahdavi, S., Kafi, M., Fallahi, E., Shokrpour, M., Tabrizi, L., 2016. Water stress, nano silica, and digoxin effects on minerals, chlorophyll index, and growth of ryegrass. Int. J. Plant Prod. 10 (2), 251–264.
Mannivannam, A., Ahn, Y.K., 2017. Silicon regulates potential genes involved in major physiological processes in plants to combat stress. Front. Plant Sci. https://doi.org/10.3389/fpls.2017.01346.
Maxwell, K., Johnson, G.N., 2000. Chlorophyll fluorescence – a practical guide. J. Exp. Bot. 51 (345), 659–668.
Miyake, C., Horiguchi, S., Makino, A., Shinzaki, Y., Yamamoto, H., Tomizawa, K., 2005. Effects of light intensity on cyclic electron flow around PSI and its relationship to non-photochemical quenching of Chl fluorescence in tobacco leaves. Plant Cell Physiol. 46, 1819–1830.
Miyake, C., 2010. Alternative electron flows (Water–Water cycle and cyclic electron flow around PSI) in photosynthesis: molecular mechanisms and physiological functions. Plant Cell Physiol. 51 (12), 1951–1963.
Mohanty, P., Allakhverdiev, S.I., Murata, N., 2007. Application of low temperatures during photoinhibition allows characterization of individual steps in photodamage and the repair of photosystem II. Photosynth. Res. 94, 217–224.
Muller, P., Xiao-Ping, L., Niyogi, K.K., 2001. Non-photochemical quenching. A response to excess light energy. Plant Physiol. 125, 1558–1566.
Neto, M.C.L., Cerqueira, J.V.A., Cunha, J.R.D., Ribeiro, R.V., Silveira, J.A.G., 2017. Cyclic electron flow, NPQ and photorespiration are crucial for the establishment of young plants of *Ricinus communis* and *Jatropha curcas* exposed to drought. Plant Biol. 19, 650–659.
Oxborough, K., Baker, N.R., 1997. Resolving chlorophyll a fluorescence images of photosynthetic efficiency into photochemical and non-photochemical components- calculation of qP and F_v'/F_m' without measuring F_o'. Photosynth. Res. 54, 135–142.
Pandey, K., Lahiani, M.H., Hicks, V.K., Hudson, M.K., Green, M.J., Khodakovskaya, M., 2018. Effects of carbon-based nanomaterials on seed germination, biomass accumulation and salt stress response of bioenergy crops. PloS One 13 (8). https://doi.org/10.1371/journal.pone.0202274.
Perez-de-Luque, 2017. Interaction of Nanomaterials with plants: what do we need for real applications in agriculture? Front. Environ. Sci| 5 (12). https://doi.org/10.3389/fenvs.2017.00012.
Qi, M., Liu, Y., Li, T., 2013. Nano-TiO2 improve the photosynthesis of tomato leaves under mild heat stress. Biol. Trace Elem. Res. 156, 323–328.
Rad, J.S., Karimi, J., Mohsenzadeh, S., Rad, M.S., Moradgholi, J., 2014. Evaluating SiO2 nanoparticles effects on developmental characteristic and photosynthetic pigment contents of *Zea mays* L. Bull Environ Pharmacol. Life Sci 3, 194–201.
Rymbai, H., Laxman, R.H., Dinesh, M.R., Sunoj, V.S.J., Ravishankar, K.V., Jha, A.K., 2014. Diversity in leaf morphology and physiological characteristics among mango (Mangifera indica) cultivars popular in different agro-climatic regions of India. Sci. Hortic 176, 189–193.
Selvarajan, D., Mohan, C., Dhandapani, V., Nerkar, G., Jayanarayanan, A., Mohanan, V., Murugan, N., Kaur, L., Chennappa1, M., Kumar, R., Meena, M., Ram, B., Chinnaswamy, A., 2018. Differential gene expression profiling through transcriptome approach of *Saccharum spontaneum* L. under low temperature stress reveals genes potentially involved in cold acclimation. 3 Biotech 8, 195.
Shi, Y., Wang, Y., Flowers, T.J., Gong, H., 2013. Silicon decreases chloride transport in rice (*Oryza sativa* L.) in saline conditions. J. Plant Growth Regul. 170, 847–853.
Siddiqui, M.H., El whaibi, M.H., Faisal, M., Al Sahli, A., 2014. Nano-silicon dioxide mitigates the adverse effects of salt stress on *Cucurbita pepo* L. Environ. Toxicol. Chem. 33 (11), 2429–2437.
Singh, A., Prasad, S.M., Singh, S., 2018. Impact of nano ZnO on metabolic attributes and fluorescence kinetics of rice seedlings. Environ. Nanotechnol Monit Manag 9, 42–49.
Singh, J., Lee, B.K., 2016. Influence of nano-TiO_2 particles on bioaccumulations of Cd in soybean plants (*Glycine max*): a possible mechanism for removal of Cd from contaminated soil. J. Environ. Manag. 170, 88–96.
Sonoike, K., 2011. Photoinhibition of photosystem I. Physiol. Plantarum 142, 56–64.
Stampoulis, D., Sinha, S.K., White, J.C., 2009. Assay-dependent phytotoxicity of nanoparticles to plants. Environ. Sci. Technol. 43, 9473–9479.
Subbaiah, L.V., Krishna, T.N., Prasad, V., Krishna, T.G., Sudhakar, P., Reddy, B., Pradeep, T., 2016. Novel effects of nanoparticulate delivery of zinc on growth, productivity and zinc bio-fortification in maize (*Zea mays* L.). J. Agric. Food Chem. 64 (19), 3778–3788.
Sunoj, V.S.J., Shroyer, K.J., Krishna, J., Prasad, V., 2016. Diurnal temperature amplitude alters physiological and biochemical response of Maize (*Zea mays*) during the vegetative stage. Environ. Exp. Bot. 130, 113–121.
Sunoj, V.S.J., Impa, M.S., Chiluwal, A., Perumal, R., Prasad, P.V.V., Krishna Jagadish, S.V., 2017. Resilience of pollen and post flowering response in diverse sorghum genotypes exposed to heat stress under field conditions. Crop Sci. 57, 1–12.
Takahashi, S., Milward, S.E., Fan, D.Y., Chow, W.S., Badger, M.R., 2009. How does cyclic electron flow alleviate photoinhibition in Arabidopsis. Plant Physiol. 149, 1560–1567.
Torabian, S., Zahedi, M., Khoshgoftar, A.H., 2017. Effects of foliar spray of nano-particles of FeSO4 on the growth and ion content of sunflower under saline condition. J. Plant Nutr. 40, 615–623.
Trenberth, K.E.P.D., Jones, P.D., Ambenje, P., et al., 2007. Observations: surface and atmospheric climate change: the physical science basis. In: Solomon, S., Qin, D., Manning, M. (Eds.), Contribution of WG 1 to the Fourth Assessment Report of the Intergovernmental Panel on Climate Change. Cambridge University Press, Cambridge, UK, pp. 235–336 2007.
Tjus, S.E., Moller, B.L., Scheller, H.V., 1998. Photosystem I is an early target of photoinhibition in barley illuminated at chilling temperature. Plant Physiol. 116, 755–764.
Wellburn, A.R., 1994. The spectral determination of chlorophylls a and b as well, as the total carotenoids using various solvents with using various solvents with spectrophotometers of different resolution. J. Plant Physiol. 144 (3), 307–313.
Yassen, A., Emam, A., Maybelle, G., Sahar, Z., 2017. Role of silicon dioxide nano fertilizer in mitigating salt stress on growth yield and chemical composition of cucumber (*Cucumis sativus* L.). Int. J. Agric. Res. 130, 135.
Zhang, M., Gao, B., Chen, J., Li, Y., 2015. Effects of graphene on seed germination and seedling growth. J. Nanoparticle Res. 17, 78.
Zidan, A., Omar, S., 2019. Nano Selenium: reduction of severe hazards of Atrazine and promotion of changes in growth and gene expression patterns *on Vicia faba* seedlings. Afr. J. Biotechnol. 18 (23), 502–510.